CrystEngComm

PAPER

View Article Online
View Journal | View Issue

Cite this: *CrystEngComm*, 2018, **20**, 6821

Different photochromic properties induced by lone pair–π interactions with varying strengths in two stereocontrolled self-assembly isomeric coordination polymers†

Chen Fu, Guo-Shuai Zhang, Hai-Yu Wang, Li Li, Jia-Wei Fu, Ya-Nan Sun and Hong Zhang *

Received 14th August 2018,
Accepted 25th September 2018

DOI: 10.1039/c8ce01367e

rsc.li/crystengcomm

Two novel cadmium-based isomeric coordination polymers constructed from naphthalenediimide chromophoric components and aromatic dicarboxylic acids, [Cd(DPMNI)(*m*-BDC)]$_n$ (**1**) and [Cd(DPMNI)(*p*-BDC)]$_n$ (**2**) (DPMNI = *N*,*N*′-bis(4-pyridylmethyl)-1,4,5,8-naphthalenediimide, *m*-BDC^{2-} = isophthalate, *p*-BDC^{2-} = terephthalate) have been synthesized by solvothermal reactions and characterized systematically. Single-crystal X-ray diffraction analyses results indicate that compounds **1**–**2** possess the same basic building block, but show different 2D resultant constructions. The formation of non-covalent intermolecular interactions (CH–π, π–π, lone pair–π interactions) can not only generate 3D supramolecular structures, but also improve structural thermostabilities up to approximately 405 °C and 330 °C, according to their thermogravimetric analyses (TGA) results. Importantly, due to the stereocontrolled self-assembly of the isomeric coordination polymers, two kinds of lone pair–π interactions with varying strengths have been produced leading to different photochromic behaviors in **1**–**2**. It is worth mentioning that the immediate photochromism of **1** is rare in NDI-based photochromic materials. Moreover, their photoluminescence properties have also been investigated to enrich the research on crystal photophysical properties.

Introduction

Redox photochromic materials derived from photoinduced electron transfer have attracted a growing number of researchers over the past few decades for the development of well-designed structures and the potential applications in photoactive devices containing optical memories,[1] magnetic switches,[2] smart windows[3] and photochromic decorations.[4] Generally, while designing a photoinduced electron transfer system, we should keep several primary factors in mind: (1) the electron-donating or accepting abilities of suitable donors and acceptors; (2) the reasonable electron transfer pathway and (3) the satisfactory distance of the pathway. For high-performance photochromic materials, the rational match between electron donors and acceptors as well as the subsequent generation of stable radicals should be considered. Naphthalenediimide derivatives (NDIs) are an attractive class of neutral, π-conjugated planar, diimide nitrogen substitution-based compounds possessing a uniform electron-deficient naphthalenediimide (NDI) center, which usually acts as electron acceptors in the electron transfer process receiving electrons to generate colored radicals.[5] As we all know, establishing a covalent connection for a fast electron transfer is an elaborate strategy traditionally.[6] However, some unconventional non-covalent intermolecular interactions such as π–π,[7] anion–π,[8] and lone pair–π interactions[9] as well as hydrogen bonding force,[10] have also been paid much attention, which can not only stabilize structures, but also support electron transfer as efficient pathways. Especially, lone pair–π interactions are promising, which can often take place between lone pair-bearing electronegative atoms (*e.g.* halogen, oxygen atoms) and electron-deficient conjugate planes. Owing to the frequent use of electron-rich solvents[9a] (*e.g.* *N*,*N*′-dimethylformamide, DMF; *N*,*N*′-dimethylacetamide, DMA; *N*-methyl-2-pyrrolidone, NMP), metallic nitrates[9b,c] or metal halides,[6a] and the fellow carboxylic ligands[11] while obtaining NDI-based materials, lone pair–π interactions are usually formed in final structures, thereby resulting in photochromic behaviors. In fact, Liu *et al.*[6a,9a] have demonstrated the impact of lone pair–π interactions on photochromic properties of NDI-based coordination networks. Likewise, Liao

---

*Institute of Polyoxometalate Chemistry, Department of Chemistry, Northeast Normal University, Changchun, Jilin 130024, PR China.
E-mail: hope20130122@163.com, zhangh@nenu.edu.cn*

† Electronic supplementary information (ESI) available: Graphics (Fig. S1–S10) and tables (Tables S1 and S2). CCDC 1585538 and 1585536. For ESI and crystallographic data in CIF or other electronic format see DOI: 10.1039/c8ce01367e

et al.[12] have reported a 2D coordination network based on TauNDI ligand, which exhibits rapid photochromic transformation in the presence of such interactions.

Recently, we have reported that three novel metal organic frameworks, based on IsoNDI ligand and three different aromatic dicarboxylic acids as the secondary building linkers, show photochromic behaviors caused by π–π and lone pair–π interactions.[11] The study has provided meaningful and valuable insights into designing interesting NDI-based photochromic materials through lone pair–π interactions. For further study, we have replaced IsoNDI with DPMNI, *N*,*N*′-bis(4-pyridylmethyl)-1,4,5,8-naphthalenediimide, and employed the two unchanged aromatic dicarboxylic acids, isophthalic acid (m-H_2BDC) and terephthalic acid (p-H_2BDC) (Fig. 1), which are often used as linkers cooperating with diamine linkers to construct porous frameworks.[13] Thus, we synthesized two new isomeric coordination polymers, $[Cd(DPMNI)(m\text{-}BDC)]_n$ (**1**) and $[Cd(DPMNI)(p\text{-}BDC)]_n$ (**2**). As expected, the two compounds are photochromic changing from yellow to brown upon irradiation using a xenon lamp (300 W, 320–780 nm) through the lone pair–π interactions. DPMNI ligands in **1** have been significantly affected by coordination environment showing greater torsion and forming stronger lone pair–π interactions with neighbouring dicarboxylic group, while DPMNI ligands in **2** have been little influenced by structural steric hindrance, thus exhibiting random arrange modes and generating weaker lone pair–π interactions with adjacent companions. Similar to that in **2**, congeneric lone pair–π interactions between adjacent IsoNDI ligands have also been observed as electron transfer pathways in reported frameworks $[Cd(IsoNDI)(m\text{-}BDC)(DMF)]_n$ and $[Cd_2(IsoNDI)_2(p\text{-}BDC)_{0.5}(MAC)_2]_n$.[11] Moreover, by contrast, the photochromic rate of **1** is the fastest because the electron-donating ability of electronegative dicarboxylic oxygen atoms with more negative charge is stronger than that of the oxygen atom from electroneutral carbonyl group of electron-deficient NDIs, which relatively contains more positive charge although the distance of the pathway in **1** is larger than those of the others. It is noteworthy that the immediate photochromic property of **1** is rare in reported NDI-based materials. This study has not only convincingly corroborated the influence of lone pair–π interactions on photochromism of NDI-based materials, but also provided a feasible idea to design rapid photoinduced electron transfer system.

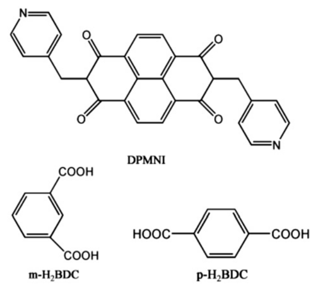

Fig. 1 Ligands adopted in the study.

Experimental section

Materials and measurements

All the chemicals and solvents were purchased commercially and used without further purification. The ligand DPMNI was synthesized according to the previously reported literature.[14] Elemental analyses (C, H and N) were performed using a PerkinElmer 2400 CHN elemental analyzer. The infrared (IR) spectra were recorded in the range of 400–4000 cm^{-1} using a Mattson Alpha-Centauri spectrometer with KBr pellets. The powder X-ray diffraction (PXRD) patterns were obtained using a Rigaku Dmax 2000 X-ray diffractometer (Cu Kα, λ = 0.15418 nm) with 2θ ranging from 5° to 50° at room temperature. Thermogravimetric analyses (TGA) data were received using a PerkinElmer thermal analyzer by heating crystalline products under nitrogen gas flow at a heating rate of 10 °C min^{-1} in the range of 30–800 °C. The solid-state UV-vis diffuse-reflectance spectra were measured using a Cary 500 UV-vis-NIR spectrophotometer in the wavelength range of 200–800 nm. Electron spin resonance (ESR) measurements were carried out at X-band frequency (9.45 GHz) using a Bruker EMX spectrometer. Meanwhile, excitation and emission spectra were recorded using a FLSP920 fluorescence spectrometer. All calculations were carried out using the Gaussian 09 program package.[15]

Synthetic procedures

A mixture of DPMNI (0.0224 g, 0.05 mmol), isophthalic acid (m-H_2BDC) or terephthalic acid (p-H_2BDC) (0.0085 g, 0.05 mmol), and Cd $(NO_3)_2$ $4H_2O$ (0.0308 g, 0.1 mmol) in DMF/H_2O (6 mL, 5 : 1) solution was stirred for 30 minutes. Then the mixtures were sealed in a 25 mL Teflon reactor autoclave and heated at 90 °C for 4 days. After cooling down to room temperature, the obtained yellow black single crystals of compounds **1–2** were collected and washed with water, and finally dried in air at room temperature.

1: yield: 17.04 mg, *ca.* 47% based on DPMNI. Anal. calcd (%) for $C_{34}H_{20}N_4O_8Cd$: C 56.33, H 2.76, N 7.73. Found: C 56.15, H 2.85, N 7.61. IR data (KBr, cm^{-1}): 3483 (w), 2100 (w), 1926 (w), 1700 (s), 1657 (s), 1604 (m), 1543 (m), 1501 (w), 1439 (m), 1379 (m), 1318 (s), 1222 (m), 1169 (m), 1065 (m), 1007 (m), 944 (w), 900 (w), 883 (m), 804 (m), 770 (s), 726 (s), 664 (m).

2: yield: 18.48 mg, *ca.* 51% based on DPMNI. Anal. calcd (%) for $C_{34}H_{20}N_4O_8Cd$: C 56.33, H 2.76, N 7.73. Found: C 56.27, H 2.87, N 7.69. IR data (KBr, cm^{-1}): 3492 (w), 2066 (w), 1909 (w), 1699 (m), 1664 (s), 1604 (m), 1552 (m), 1500 (w), 1447 (m), 1371 (m), 1325 (s), 1228 (m), 1181 (m), 1066 (m), 1005 (m), 936 (w), 909 (w), 876 (m), 838 (w), 807 (m), 768 (s), 726 (s), 655 (m).

X-ray diffraction analyses

Suitable single crystals of compounds **1–2** were selected for single-crystal X-ray diffraction analyses using an Oxford Diffraction Gemini R Ultra diffractometer with graphitemonochromated Mo-Kα radiation (λ = 0.71073 Å) at 296 K. Absorption corrections were applied using the multiscan technique. The structures of **1–2** were solved by the direct method followed by the difference and further refined with a full-matrix least-squares technique using the program package of SHELXTL-2014/1.[16] Thermal parameters of all non-H atoms of crystals were refined with anisotropic temperature parameters, and H atoms on organic ligands were fixed at calculated positions. The detailed crystallographic data and structure refinement parameters of **1–2** are summarized in Table S1.† Selected bond lengths and angles of **1–2** are listed in Table S2.† Crystallographic data were deposited at the Cambridge Crystallographic Data Center (CCDC) with supplementary publication numbers CCDC 1585538 1585536 for **1–2**, respectively.

Results and discussion

Description of the crystal structures

The single-crystal X-ray diffraction study shows that compound **1** crystallizes in the orthorhombic space group *Pnma*, and the asymmetric unit consists of half a crystallographically independent Cd cation, half a DPMNI ligand and half a *m*-BDC^{2-} ligand. As shown in Fig. 1a, each Cd center is hexacoordinated by four O atoms from two bidentate-coordinated *m*-BDC^{2-} ligands with Cd–O distances of 2.266–2.512 Å and two N atoms from two DPMNI ligands with Cd–N distances of 2.254–2.255 Å. The dihedral angles between the planes of the NDI center and marginal pyridine rings in the DPMNI ligand are 68.69, 89.78, 70.19 and 89.6°, which are comparable to those in previously reported DPMNI-based compounds.[17] The neighbouring two Cd cations are bridged by DPMNI ligands with a distance of 13.7203 Å to form an infinite 1D S-shaped coordination polymer, in which DPMNI ligands with a non-planar structure present two kinds of patterns that can be distinctly described as peak (red) and valley (orange) (Fig. 2b). The adjacent two 1D coordination polymers are connected to each other through *m*-BDC^{2-} ligands with μ^2: $\eta^1\eta^1\eta^1\eta^1$ mode that link with Cd^{2+} cations generating 2D coordination networks (Fig. 2c and S1a†), which contain two directional developments, as shown in Fig. 2d and S1.† Besides, the structures are further stabilized by CH–π and lone pair–π interactions between DPMNI ligands and adjacent *m*-BDC^{2-} ligands (2.947 and 3.250 Å, 3.484 Å, Fig. 4) producing a three-dimensional structure (Fig. S2†), which can be supported by TGA result revealing that compound **1** exhibits excellent thermal stability up to 405 °C (Fig. S9a†).

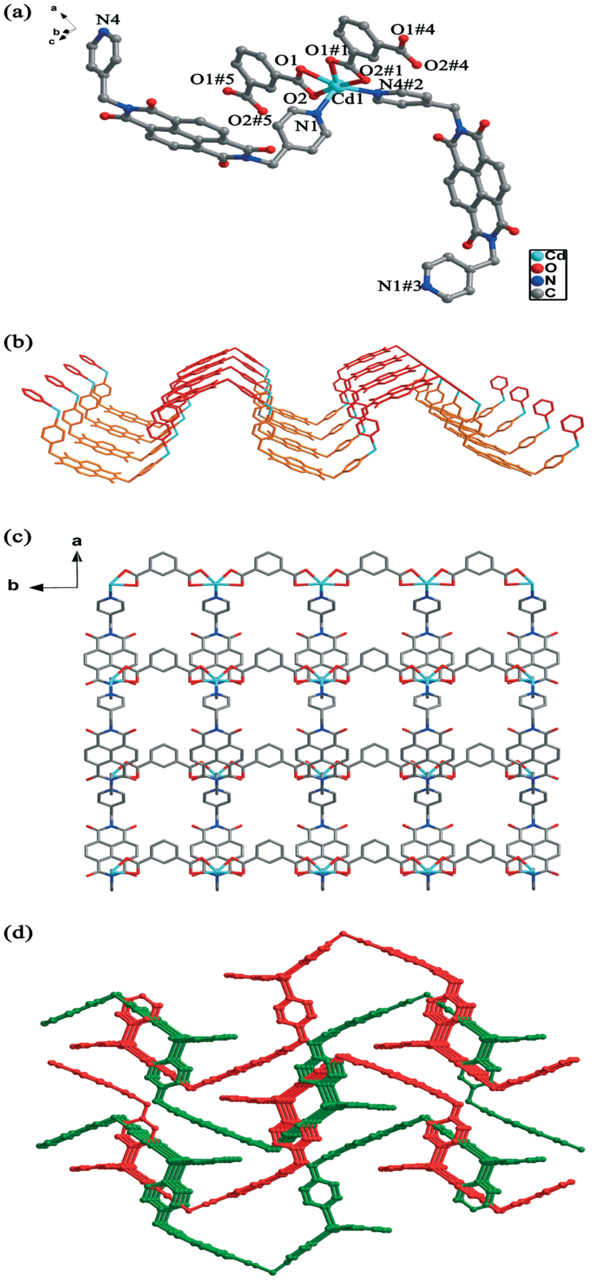

Fig. 2 (a) The coordination environment of Cd cation in compound **1**; (b) 1D polymers contained in structure of **1** built from the predesigned ligand DPMNI and Cd cation; (c) the 2D coordination networks and (d) the packing diagram of the two directional developments in 2D networks. All H atoms were removed for clarity. Symmetry code: #1, *x*, 0.5 − *y*, *z*; #2, −0.5 + *x*, *y*, 0.5 − *z*; #3, 0.5 + *x*, 0.5 − *y*, 0.5 − *z*; #4, *x*, −1 + *y*, *z*; #5, *x*, 1.5 − *y*, *z*.

Compound **2** crystallizes in the monoclinic space group *P*21/*n*, and the asymmetric unit contains one Cd cation, one DPMNI ligand and two half *p*-BDC^{2-} ligands. Cd1 center exhibits a slightly distorted octahedral geometry coordinated by four O atoms from two *p*-BDC^{2-} ligands with Cd–O distances of 2.298–2.430 Å and two N atoms from two DPMNI ligands with Cd–N distances of 2.294–2.313 Å (Fig. 3a). The dihedral angles between the planes of the NDI center and marginal pyridine rings in the DPMNI ligand are 76.47, 78.33, 78.85 and 76.03°, which are approximately equal with each other suggesting that the companionate *p*-BDC^{2-} ligand has little effect on the geometry of DPMNI ligand because 1,4-disubstituted *p*-H$_2$BDC has smaller steric hindrance compared with 1,3-disubstituted *m*-H$_2$BDC. The four ligands in basic unit grow outward keeping their own coordination regularities, thus forming repetitive units to generate an open 2D coordination polymer (Fig. 3c) where independent (Cd-

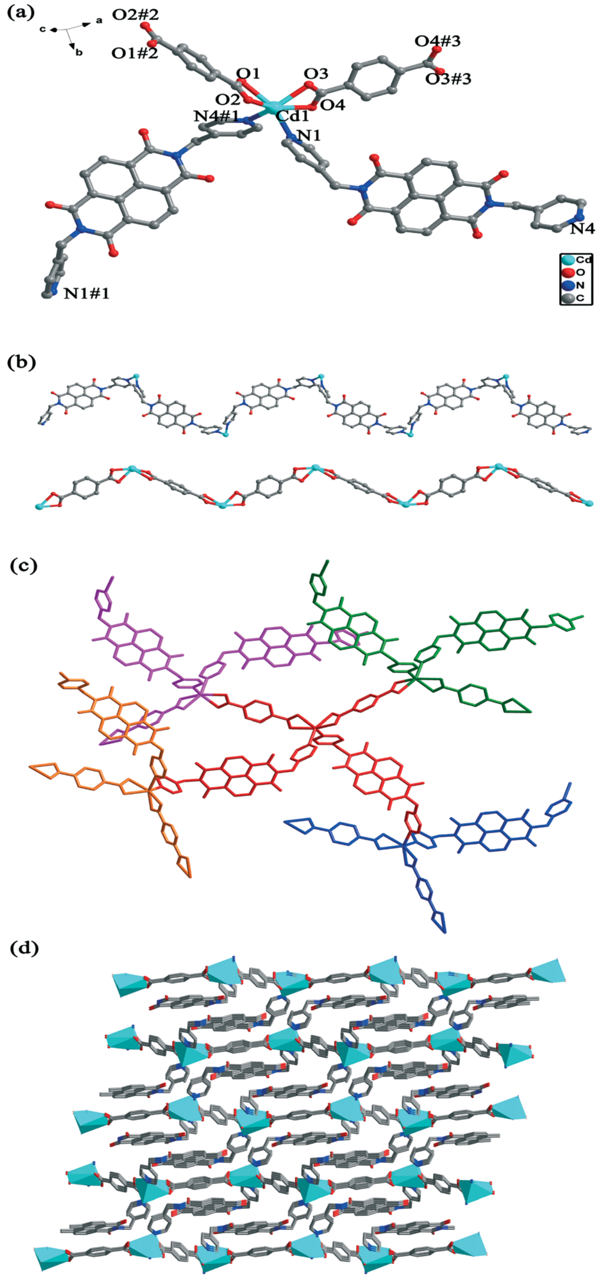

Fig. 3 (a) The coordination environment of Cd cation in compound **2**. (b) (Cd-DPMNI)$_\infty$ and [Cd-(p-BDC)]$_\infty$ 1D zigzag-shaped polymers, respectively, in **2**. (c) One fundamental building block (red) and its surrounding four kinds of extended modes (green, orange, pink and blue). (d) The packing diagram along one precise direction. All H atoms were removed for clarity. Symmetry code: #1, −0.5 + x, 1.5 − y, 0.5 + z; #2, −x, −1 − y, 1 − z; #3, 1 − x, −y, 1 − z.

DPMNI)$_\infty$ and [Cd-(p-BDC^{2-})]$_\infty$ 1D coordination polymers all present a zigzag-shaped appearance (Fig. 3b). Interestingly, CH–π and lone pair–π interactions are observed between neighbouring DPMNI ligands (Fig. 5a), which can stabilize the structure efficiently. Apart from above two kinds of interactions, there are π–π stacking interactions between the benzene ring of p-BDC^{2-} ligand and the adjacent pyridine ring or NDI center of DPMNI ligand, as shown in Fig. 5b and c. Subsequently, the π–π stacking interactions between the benzene ring and the pyridine ring with distances of approximately 3.388 and 3.423 Å overlap with each other by about 33.3%, while other π–π stacking interactions between benzene ring and NDI center with distances approximately ranging from 3.352 to 3.531 Å overlap almost face-to-face. The formation of such π–π stacking interactions further strengthens structural stability. The TGA result indicates that the structure is stable up to approximately 330 °C.

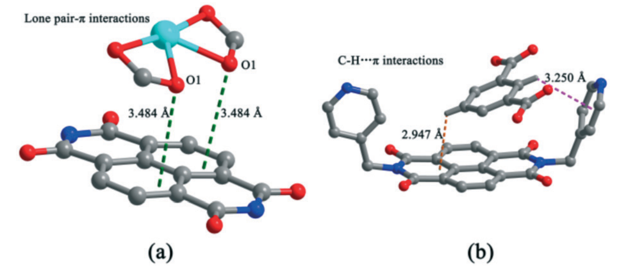

Fig. 4 (a) Lone pair–π interactions between isophthalate and neighbouring NDI center of DPMNI ligand and (b) C–H···π interactions between benzene ring of m-BDC^{2-} ligand and neighbouring NDI center or pyridine ring of DPMNI ligand in compound **1**.

Photochromic properties and mechanism

We have reported that the three naphthalenediimide-based metal organic frameworks are reversible light-induced color-changed structures. Herein, photochromic properties of compounds **1–2** were also examined in air at room temperature. As a result, upon irradiation (xenon lamp, 300 W, 320–780 nm), **1** can rapidly turn from yellow (**1a**) to dark brown (**1b**) in 1 second, while **2** can turn from yellow (**2a**) to brown (**2b**) in 30 seconds, and their discoloration saturation times are 5 and 20 minutes, respectively (Fig. 6). The photochromic products **1b** and **2b** are stable in air but can restore initial colors after being in a dark room for about one month at room temperature, which suggests that photochromic behaviors of **1–2** are reversible. To understand the reason behind their

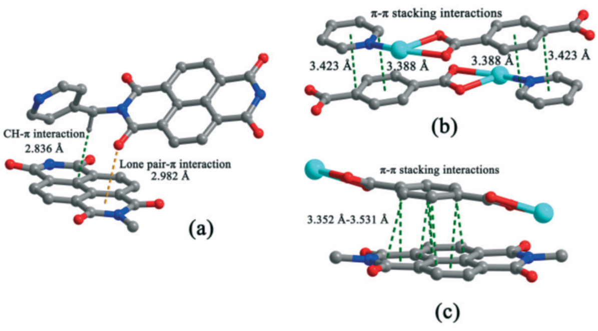

Fig. 5 (a) Lone pair–π and C–H···π interactions among neighbouring DPMNI ligands and (b) part-to-part π–π interactions between the benzene ring of p-BDC^{2-} ligand and the neighbouring pyridine ring of DPMNI ligand and (c) face-to-face π–π interactions between benzene ring of p-BDC^{2-} ligand and neighbouring NDI center of DPMNI ligand in compound **2**.

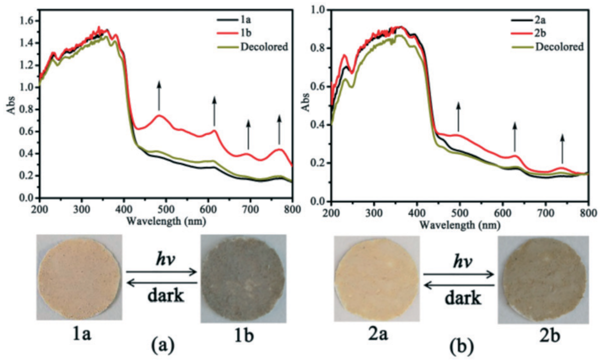

Fig. 6 UV-vis spectra and photographs showing photochromic behaviors of compounds **1** (a)-**2** (b). Inset: **1a**, **2a**: before irradiation; **1b**, **2b**: after irradiation using a 300 W xenon lamp; decolored: irradiated samples were disposed by dark treatment for about a month.

photochromic behavior, UV-vis diffuse-reflectance spectroscopy and electron spin resonance (ESR) measurements have been carried out during photochromic processes. As shown in Fig. 6, the UV-vis studies display that upon irradiation the major influence on **1**–**2** is not the enhanced broad absorption bands in the region of 200–400 nm that are ascribed to the typical π–π* and *n*–π* transition of conjugated aromatic rings,[18] but rather the appearance of new bands in the region of 400–800 nm, where there are two intrinsic absorption bands at 615 and 767 nm that result from being too sensitive to natural light and two new absorption bands at 485 and 693 nm in **1b**, while an intrinsic band at 627 nm and two new bands at 500 and 735 nm in **2b**. Previous studies of NDIs have mentioned that these absorption bands are attributed to the formation of NDIs radicals caused by photoinduced electron transfer, which can be supported by ESR studies. As depicted in Fig. 7, original samples **1a** and **2a** have no ESR signals primarily, but irradiated samples **1b** and **2b** exhibit distinct single-line signals with $g = 2.0035$ and 2.0041, which are close to that of a free electron (2.0023) confirming the formation of DPMNI radicals. Besides, the unchanged PXRD and IR spectra before and after irradiation further prove that such photoresponsive behaviors are not resulting from structural transformation or photolysis (Fig. S7 and S8†). It is well known that the quantity of radicals is directly proportional to the amount of transferred electron, when we increase the irradiation time, the intensities of those absorption bands gradually increase, which is consistent with gradually deepening colors (Fig. S4†).

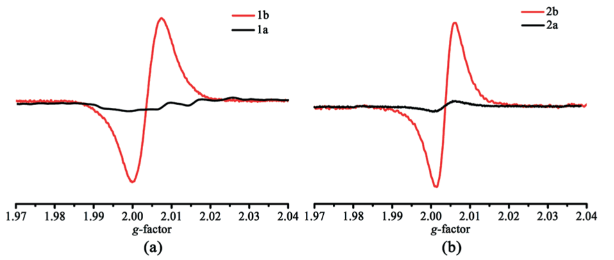

Fig. 7 ESR spectra of compounds **1** (a) and **2** (b) before and after irradiation using a 300 W xenon lamp.

As summarized above, some non-covalent interactions can be useful pathways to support electron transfer. Structural analysis of compound **1** exhibits that there are lone pair–π interactions with the shortest distance of 3.484 Å between m-BDC^{2-} ligand and neighbouring DPMNI ligand, as shown in Fig. 4a. From our previous study,[11] frameworks [Cd(IsoNDI)(m-BDC)(DMF)]$_n$ and [Cd$_2$(IsoNDI)$_2$ (p-BDC)$_{0.5}$(MAC)$_2$]$_n$ all possess reversible photochromic properties induced by lone pair–π interactions with distances of 3.098 Å and 3.278 Å between neighbouring IsoNDI ligands (Fig. S3b and c†). Comparing the above reported two frameworks and **1**, **1** changes color more rapidly, which can be called immediate photochromism. As we all know, the electron-donating/accepting abilities are key factors for photochromic property. In the lone pair–π interactions formed between them, the same electron-deficient NDI centers act as electron-accepting tectons, but electron-donating oxygen atoms belong to different components where the contributing oxygen atoms show that electronegativity in **1** is from electron-rich isophthalate, while those in the two frameworks are from electroneutral carbonyl groups of electron-deficient IsoNDI molecules that possess more positive charge. Although the pathway distance of **1** (3.484 Å) is larger than those of the frameworks (3.098 Å and 3.278 Å), the electron-donating ability seems to be the leading factor for the resulting photochromism.

As for compound **2**, part-to-part and face-to-face π–π stacking interactions with distances ranging from 3.352 Å to 3.531 Å have been observed between the benzene ring of p-BDC^{2-} ligand and the adjacent pyridine rings or NDI center of DPMNI ligand. According to the case of framework [Cd(IsoNDI)(2,6-NDC)(H$_2$O)$_2$]$_n$ (ref. 11) (Fig. S3a†), such π–π stacking interactions in **2** are suitable theoretically for photoinduced electron transfer reactions. However, we have also found a kind of lone pair–π interaction with a short distance of 2.982 Å between neighbouring DPMNI ligands that can also be the leading pathway. To understand which the electron transfer pathway is or whether the effect between them is synergistic, we irradiated free DPMNI ligand with the same light condition. Because of the use of DMF solvent in the preparation process of DPMNI ligand, we heated the obtained DPMNI powder to 180 °C in order to eliminate the interference of free DMF molecules. As a result, DPMNI powder changed from pale yellow to brown (Fig. S5†). Meanwhile, the UV-vis spectrum of irradiated DPMNI sample shows two new absorption bands at 503 and 735 nm and an intrinsic band at 632 nm, which are close to those that appeared in **2b**, illustrating that photoinduced electron transfer pathways of **2** and DPMNI ligand are identical. Inspection into DPMNI structure suggests that the involved contributing pathway can only be the lone pair–π interaction between neighbouring DPMNI ligands. According to the above analysis, the pathway for electron transfer of **2** is not π–π stacking interactions, but rather lone pair–π interactions. In this way, it can be

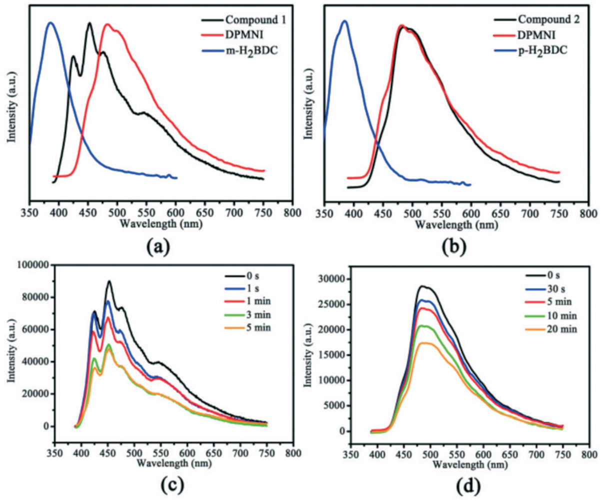

Fig. 8 Comparison of emission spectra of ligands with compounds **1** (a) and **2** (b), respectively; luminescence changes of **1** (c) and **2** (d) upon irradiation using a 300 W xenon lamp.

explained legitimately that the photoresponse rate of 2 is slower than that of **1**. To further theoretically compare the electron-donating abilities of oxygen atoms from carboxyl and carbonyl groups, NBO calculation analyses[19] for **1–2** have been carried out. As shown in Fig. S10,† the charges on isophthalic oxygen atoms (O1, −0.515, −0.518) are more negative than those on carbonyl oxygen atoms (O6, −0.425) demonstrating that the electron-donating ability of O1 is stronger than that of O6 indeed.

Photoluminescence properties

It is well known that d^{10} metal-based coordination compounds have outstanding luminescence properties.[20] The fluorescent properties of compounds **1–2** and three employed ligands have been investigated in the solid states at room temperature. As shown in Fig. 8a and b, **1** exhibits three emission peaks at 424, 452 and 475 nm (λ_{ex} = 380 nm), which show large red shifts compared with *m*-H$_2$BDC ligand emission (λ_{em} = 385 nm, λ_{ex} = 335 nm) and blue shifts compared with DPMNI ligand (λ_{em} = 484 nm, λ_{ex} = 350 nm). Meanwhile, **2** exhibits an emission peak at 484 nm (λ_{ex} = 350 nm) showing a large red shift compared with p-H$_2$BDC ligand emission (λ_{em} = 384 nm, λ_{ex} = 335 nm), but almost coinciding with DPMNI ligand emission completely, which combines with the influence of DPMNI ligand on photochromic property of **2**, thus illustrating that the DPMNI ligand plays a considerable role in physical properties of **2**. These emission peaks could be attributed to the ligand-to-metal charge transfer (LMCT).[21] In addition, crystal fluorescent properties can also be modulated by photoirradiation owing to the transfer of intermolecular electrons. The fluorescence intensities of **1–2** were gradually reduced upon irradiation using a 300 W xenon lamp and reached approximately 52.2% and 60.8% of original values in their individual photochromism saturation in 5 and 20 minutes (Fig. 8c and d).

Conclusions

In summary, we have synthesized two DPMNI ligand-based isomeric coordination polymers exhibiting different photochromic behaviors owing to different electron-donating abilities of oxygen atoms in the formed lone pair–π interactions. Compound **1** shows rare and excellent photochromic property, while compound **2** displays photophysical properties resembling those of free DPMNI ligand including photochromism and photoluminescence. Moreover, we prepared the two polymers in comparison with the previously reported three frameworks to analyze the cause of photochromism difference. We have drawn a conclusion that the electron-donating ability of donors is a noticeable factor for electron transfer efficiency, and lone pair–π interaction is a preferred pathway to support photoinduced electron transfer from our studies. We believe that our study can offer a reference to design worthy photochromic materials by selecting suitable electron-donors/acceptors and constructing a reasonable electron transfer system.

Conflicts of interest

There are no conflicts to declare.

Acknowledgements

We gratefully acknowledge financial support from the NSF of China (21571032 21271038), the China High-Tech Development 863 program (2007AA03Z218) and the analysis and testing foundation of Northeast Normal University.

Notes and references

1 (*a*) E. Zahavy and I. Willner, *J. Am. Chem. Soc.*, 1996, **118**, 12499; (*b*) C.-Z. Yu, B. Liu and L.-Q. Hu, *J. Org. Chem.*, 2001, **66**, 919; (*c*) H. Ke, L. Wang, Y. Chen, M.-J. Lin and J.-Z. Chen, *J. Mol. Catal. A: Chem.*, 2014, **385**, 26; (*d*) D. Liu, Z.-G. Ren, H.-X. Li, J.-P. Lang, N.-Y. Li and B. F. Abrahams, *Angew. Chem., Int. Ed.*, 2010, **49**, 4767; (*e*) Y.-Y. Fang, W.-J. Gong, X.-J. Shang, H.-X. Li, J. Gao and J.-P. Lang, *Dalton Trans.*, 2014, **43**, 8282; (*f*) F.-L. Hu, S.-L. Wang, J.-P. Lang and B. F. Abrahams, *Sci. Rep.*, 2014, **4**, 6815.

2 (*a*) C. Bechinger, S. Ferrere, A. Zaban, J. Sprague and B. A. Gregg, *Nature*, 1996, **383**, 608; (*b*) P. R. Andres and U. S. Sohubert, *Adv. Mater.*, 2004, **16**, 1043; (*c*) O. Sato, J. Tao and Y.-Z. Zhang, *Angew. Chem., Int. Ed.*, 2007, **46**, 2152; (*d*) F.-L. Hu, H.-F. Wang, D. Guo, H. Zhang, J.-P. Lang and J. E. Beves, *Chem. Commun.*, 2016, **52**, 7990; (*e*) N.-Y. Li, D. Liu, Z.-G. Ren, C. Lollar, J.-P. Lang and H.-C. Zhou, *Inorg. Chem.*, 2018, 57, 849; (*f*) N.-Y. Li, D. Liu, B. F. Abrahams and J.-P. Lang, *Chem. Commun.*, 2018, **54**, 5831.

3 (*a*) G. Poneti, M. Mannini, L. Sorace, P. Sainctavit, M. A. Arrio, E. Otero, J. C. Cezar and A. Dei, *Angew. Chem., Int. Ed.*, 2010, **49**, 1954; (*b*) J. Wu, C. Tao, Y. Li, Y. Yan, J. Li and J. Yu, *Chem. Sci.*, 2014, **5**, 4237; (*c*) P.-X. Li, M.-S. Wang, M.-J. Zhang, C.-S. Lin, L.-Z. Cai, S.-P. Guo and G.-C. Guo, *Angew. Chem., Int. Ed.*, 2014, **53**, 11529.

4 R. Pardo, M. Zayat and D. Levy, *Chem. Soc. Rev.*, 2011, **40**, 672.

5 (*a*) S. V. Bhosale, C. H. Jani and S. J. Langford, *Chem. Soc. Rev.*, 2008, **37**, 331; (*b*) M. Pan, X.-M. Lin, G.-B. Li and C.-Y. Su, *Coord. Chem. Rev.*, 2011, **255**, 1921; (*c*) M. A. Kobaisi, K. Latham, A. M. Raynor and S. V. Bhosale, *Chem. Rev.*, 2016, **116**, 11685; (*d*) A. Mallick, B. Garai, M. A. Addicoat, P. S. Petkov, T. Heinec and R. Banerjee, *Chem. Sci.*, 2015, **6**, 1420; (*e*) C. F. Leong, B. Chan, T. B. Faust and D. M. D' Alessandro, *Chem. Sci.*, 2014, **5**, 4724.

6 (*a*) J.-J. Liu, Y.-F. Guan, Y. Chen, M.-J. Lin, C.-C. Huang and W.-X. Dai, *Dalton Trans.*, 2015, **44**, 17312; (*b*) N. Sakai, J. Mareda, E. Vauthey and S. Matile, *Chem. Commun.*, 2010, **46**, 4225; (*c*) S. Kumar, M. R. AjayaKumar, G. Hundal and P. Mukhopadhyay, *J. Am. Chem. Soc.*, 2014, **136**, 12004; (*d*) S. V. Bhosale and S. K. Bhargava, *Org. Biomol. Chem.*, 2012, **10**, 6455.

7 (*a*) J.-Z. Liao, C. Wu, X.-Y. Xu, S.-Q. Deng and C.-Z. Lu, *Chem. Commun.*, 2016, **52**, 7394; (*b*) B. Garai, A. Mallick and R. Banerjee, *Chem. Sci.*, 2016, **7**, 2195; (*c*) H. T. Black and D. F. Perepichka, *Angew. Chem., Int. Ed.*, 2014, **53**, 2138; (*d*) J.-P. Lang, Q.-F. Xu, R.-X. Yuan and B. F. Abrahams, *Angew. Chem., Int. Ed.*, 2004, **43**, 4741; (*e*) W.-H. Zhang, Z.-G. Ren and J.-P. Lang, *Chem. Soc. Rev.*, 2016, **45**, 4995; (*f*) Y.-X. Shi, W.-X. Li, H.-H. Chen, D. J. Young, W.-H. Zhang and J.-P. Lang, *Chem. Commun.*, 2017, **53**, 5515.

8 (*a*) J.-J. Liu, Y.-F. Guan, C. Jiao, M.-J. Lin, C.-C. Huang and W.-X. Dai, *Dalton Trans.*, 2015, **44**, 5957; (*b*) J.-J. Liu, Y. Wang, Y.-J. Hong, M.-J. Lin, C.-C. Huang and W.-X. Dai, *Dalton Trans.*, 2014, **43**, 17908; (*c*) J.-Z. Liao, X.-Y. Wu, J.-P. Yong, H.-L. Zhang, W.-B. Yang, R.-M. Yu and C.-Z. Lu, *Cryst. Growth Des.*, 2015, **15**, 4952; (*d*) J.-Z. Liao, X.-J. Dui, H.-L. Zhang, X.-Y. Wu and C.-Z. Lu, *CrystEngComm*, 2014, **16**, 10530–10533.

9 (*a*) J.-J. Liu, Y.-J. Hong, Y.-F. Guan, M.-J. Lin, C.-C. Huang and W.-X. Dai, *Dalton Trans.*, 2015, **44**, 653; (*b*) C. R. Pfeiffer, N. Biggins, W. Lewis and N. R. Champness, *CrystEngComm*, 2017, **19**, 5558; (*c*) X. Fang, X. Yuan, Y.-B. Song, J.-D. Wang and M.-J. Lin, *CrystEngComm*, 2014, **16**, 9090; (*d*) Y. Chen, J.-J. Liu, C.-R. Fan, J.-Q. Li and M.-J. Lin, *Sci. China: Chem.*, 2016, **59**, 1492.

10 Z.-W. Chen, G. Lu, P.-X. Li, R.-G. Lin, L.-Z. Cai, M.-S. Wang and G.-C. Guo, *Cryst. Growth Des.*, 2014, **14**, 2527.

11 C. Fu, H.-Y. Wang, G.-S. Zhang, L. Li, Y.-N. Sun, J.-W. Fu and H. Zhang, *CrystEngComm*, 2018, **20**, 4849–4856.

12 J.-Z. Liao, J.-F. Chang, L.-Y. Meng, H.-L. Zhang, S.-S. Wang and C.-Z. Lu, *Chem. Commun.*, 2017, **53**, 9701.

13 (*a*) Y. Takashima, S. Furukawa and S. Kitagawa, *CrystEngComm*, 2011, **13**, 3360; (*b*) Y.-X. Sun and W.-Y. Sun, *CrystEngComm*, 2015, **17**, 4045.

14 P. H. Dinolfo, M. E. William, C. L. Stem and J. T. Hupp, *J. Am. Chem. Soc.*, 2004, **126**, 12989.

15 M. J. Frisch, G. W. Trucks, H. B. Schlegel, G. E. Scuseria, M. A. Robb, J. R. Cheeseman, G. A. Petersson, H. Nakatsuji, M. Caricato, J. Z. Sonnenberg, X. Li and D. J. Fox, *Gaussian 09, Revision D.01*, Gaussian, Inc., Wallingford, CT, 2013.

16 G. Sheldrick, *Acta Crystallogr., Sect. A: Found. Crystallogr.*, 2008, **64**, 112.

17 (*a*) G.-B. Li, Q.-Y. Yang, R.-K. Pan, S.-G. Liu and Y.-W. Xu, *New J. Chem.*, 2017, **41**, 6160; (*b*) J.-J. Liu, Y. Dong, L.-Z. Chen, L. Wang, S.-B. Xia and C.-C. Huang, *Acta Crystallogr., Sect. C: Cryst. Struct. Commun.*, 2018, **74**, 94; (*c*) J.-Z. Liao, X.-Y. Wu, J.-P. Yong, H.-L. Zhang, W.-B. Yang, R.-M. Yu and C.-Z. Lu, *Cryst. Growth Des.*, 2015, **15**, 4952.

18 (*a*) J.-Z. Liao, H.-L. Zhang, S.-S. Wang, J.-P. Yong, X.-Y. Wu, R.-M. Yu and C.-Z. Lu, *Inorg. Chem.*, 2015, **54**, 4345; (*b*) J. Wang, S.-L. Li and X.-M. Zhang, *ACS Appl. Mater. Interfaces*, 2016, **8**, 24862; (*c*) J.-J. Liu, S.-B. Xia, Y.-L. Duan, T. Liu, F.-X. Cheng and C.-K. Sun, *Polymer*, 2018, **10**, 165.

19 (*a*) A. E. Reed, R. B. Weinstock and F. Weinhold, *J. Chem. Phys.*, 1985, **83**, 735; (*b*) E. D. Glendening, C. R. Landis and F. Weinhold, *WIREs Comput. Mol. Sci.*, 2012, **2**, 1; (*c*) E. D. Glendening, C. R. Landis and F. Weinhold, *J. Comput. Chem.*, 2013, **34**, 1429.

20 (*a*) Z.-Q. Liu, Y. Zhao, X.-D. Zhang, Y.-S. Kang, Q.-Y. Lu, M. Azam, S. I. Al-Resayes and W.-Y. Sun, *Dalton Trans.*, 2017, **46**, 13943; (*b*) Y. Deng, Z.-Y. Yao, P. Wang, Y. Zhao, Y.-S. Kang, M. Azam, S. I. Al-Resayes and W.-Y. Sun, *RSC Adv.*, 2017, **7**, 44639.

21 (*a*) L. Han, L.-P. Xu, L. Qin, W.-N. Zhao, X.-Z. Yan and L. Yu, *Cryst. Growth Des.*, 2013, **13**, 4260; (*b*) L. Han, L. Qin, L.-P. Xu and W.-N. Zhao, *Inorg. Chem.*, 2013, **52**, 1667.